Dual Role of Mitochondrial Reactive Oxygen Species in Hypoxia Signaling: Activation of Nuclear Factor-κB via c-SRC– and Oxidant-Dependent Cell Death

Josep M. Lluis,[1] Francesca Buricchi,[2] Paola Chiarugi,[2] Albert Morales,[1] and José C. Fernandez-Checa[1]

[1]Liver Unit, Centro de Investigaciones Biomédicas Esther Koplowitz, Instituto de Malalties Digestives, Hospital Clinic I Provincial and CIBEREHD, Instituto Salud Carlos III, University of Barcelona, IDIBAPS and Department of Cell Death and Proliferation, Instituto Investigaciones Biomédicas, Consejo Superior Investigaciones Científicas, Barcelona, Spain and [2]Department of Biochemical Sciences, Faculty of Medicine and Surgery, University of Florence, Florence, Italy

Abstract

Hypoxia is a prominent feature of solid tumor development and is known to stimulate mitochondrial ROS (mROS), which, in turn, can activate hypoxia-inducible transcription factor-1α and nuclear factor-κB (NF-κB). Because NF-κB plays a central role in carcinogenesis, we examined the mechanism of mROS-mediated NF-κB activation and the fate of cancer cells during hypoxia after mitochondrial reduced glutathione (mGSH) depletion. Hypoxia generated mROS in hepatoma (HepG2, H35), neuroblastoma (SH-SY5Y), and colon carcinoma (DLD-1) cells, leading to hypoxia-inducible transcription factor-1α–dependent gene expression and c-Src activation that was prevented in cells expressing a redox-insensitive c-Src mutant (C487A). c-Src stimulation activated NF-κB without IκB-α degradation due to IκB-α tyrosine phosphorylation that was inhibited by rotenone/TTFA or c-Src antagonism. The c-Src–NF-κB signaling contributed to the survival of cells during hypoxia as c-Src inhibition or p65 down-regulation by small interfering RNA–sensitized HepG2 cells to hypoxia-induced cell death. Moreover, selective mGSH depletion resulted in an accelerated and enhanced mROS generation by hypoxia that killed SH-SY5Y and DLD-1 cells without disabling the c-Src–NF-κB pathway. Thus, although mROS promote cell survival by NF-κB activation via c-Src, mROS overgeneration may be exploited to sensitize cancer cells to hypoxia. [Cancer Res 2007;67(15):7368–77]

Introduction

Hypoxia is an inherent and key feature of solid tumor development that arises due to the disorganized structure and architecture of tumor vasculature resulting in irregular and inefficient oxygen delivery, and is considered a negative prognostic factor for response to treatment and survival of cancer patients (1–3). A central pathway in oxygen sensing that mediates the gene expression reprogramming and the adaptation to this stressful condition is the hypoxia-inducible transcription factor 1 (HIF-1), a heterodimer transcription factor comprised by α and β subunits, which induces a cadre of genes that promote angiogenesis, survival, glycolysis, and tumor progression (4–6). Although the β subunit is constitutively expressed, the expression of the HIF-1α subunits is tightly regulated by oxygen through the action of prolyl hydroxylase (PHD) and asparaginyl hydroxylase (7–10). In the presence of oxygen, iron, or 2-oxoglutarate, PHDs hydroxylate specific proline residues within the oxygen-dependent domain of HIF-1α, enabling its binding to the von Hippel-Landau tumor suppressor protein, a component of the E3 ubiquitin ligase complex that leads to the ubiquitination and subsequent proteasome-dependent degradation of HIF-1α subunits (10–12). PHDs belong to the iron (II)-2-oxoglutarate–dependent dioxygenase family and are thought to be effective oxygen sensors as their K_m values for oxygen are above the atmospheric oxygen concentration (13).

In addition to the role of PHDs as oxygen sensors, an alternative model proposes mitochondria as critical players in oxygen sensing through inhibition of PHDs. This mitochondrial model, however, has been controversial because previous studies relied on pharmacologic tools with the appearance of conflicting reports (14, 15) and also due to technical concerns regarding the measurement of ROS production in living cells. However, recent studies using genetic and biochemical approaches have provided clear-cut evidence for a role of mitochondrial reactive oxygen species (mROS) in oxygen sensing and HIF-1α activation (16–18). Indeed, blocking superoxide anion production by suppressing the Rieske iron-sulfur protein of complex III impairs HIF-1α induction by hypoxia, and, moreover, hydrogen peroxide or agents that produce ROS activate HIF-1α during normoxia (17, 18), indicating a central role for ROS in the stabilization of HIF-1α. Furthermore, hypoxia-induced mROS have been shown to enhance the DNA binding of nuclear factor-κB (NF-κB) through a redox-dependent mechanism (19). The prototypical pathway leading to NF-κB activation by a wide variety of stimuli involves the phosphorylation of IκB at specific serine residues that targets its subsequent degradation by the proteasome (20–22). The released subunits of NF-κB then translocate to the nucleus where they bind to specific sites in the promoter/enhancer region of target genes. An additional pathway of NF-κB activation entails the release of the DNA binding–competent dimers of NF-κB from IκB-α without the proteolytic degradation of the latter. Indeed, the phosphorylation of IκB-α at tyrosine residues has been shown to activate NF-κB without IκB-α degradation (23).

Compared with HIF-1α, the regulation of NF-κB during hypoxia has been less studied, and although the phenomenon was observed in the past, the molecular mechanisms involved remained unclear. In this regard, hypoxia (0.02% O_2) has been reported to activate NF-κB through the phosphorylation of IκB-α on tyrosine residues;

Note: Supplementary data for this article are available at Cancer Research Online (http://cancerres.aacrjournals.org/).

A. Morales and J.C. Fernández-Checa share senior authorship.

Requests for reprints: José C. Fernández-Checa, Liver Unit, Institut of Malalties Digestives, Hospital Clinic i Provincial, C/ Villarroel, 170, 08036 Barcelona, Spain. Phone: 34-93-451-5272; Fax: 34-93-451-5272; E-mail: checa229@yahoo.com.

doi:10.1158/0008-5472.CAN-07-0515

however, this outcome was accompanied by the proteolytic degradation of IκB-α (24). Furthermore, Imbert et al. reported that hypoxia failed to phosphorylate IκB-α in tyrosine residues as opposed to hypoxia/reoxygenation or pervanadate, which activated NF-κB in the absence of IκB-α degradation (23, 25). Moreover, hypoxia/reoxygenation in HeLa cells induced the phosphorylation of IκB-α on tyrosine residues and NF-κB activation through c-Src activation, a redox-regulated tyrosine kinase, that were prevented by extramitochondrial antioxidant enzymes but not by manganese superoxide dismutase (MnSOD) overexpression (26).

Given the central role of NF-κB and hypoxia in cell survival and carcinogenesis, and because the functional relation between mROS–c-Src–NF-κB during hypoxia has not been established, our aim was first to characterize the mechanisms of mROS-mediated NF-κB activation by hypoxia. Moreover, because mitochondrial reduced glutathione (mGSH) has been shown to modulate the hepatocellular susceptibility to tumor necrosis factor (TNF)/Fas or hypoxia via mROS regulation (27–29), we examined the regulation of c-Src and NF-κB after mGSH depletion and the sensitivity of cancer cells to hypoxia. Our findings reveal a dual role of mROS generated during hypoxia, promoting either cell survival through NF-κB activation via c-Src or cell death if overgenerated, suggesting that strategies to stimulate mROS production may be exploited therapeutically to turn the hypoxic environment of solid tumors into an armamentarium to kill cancer cells.

Materials and Methods

Reagents, antibodies, and plasmids. Rotenone, TTFA, sodium orthovanadate, sucrose, and Igepal CA-360 were obtained from Sigma Chemical Co. dihydro-dichlorofluorescein (DCF) diacetate and hydroethidine were obtained from Molecular Probes; MnTBAP, 4-amino-5-(4-chlorophenyl)-7-(*t*-butyl)pyrazole[3, 4-*d*]pyrimidine (PP2), and piceatannol were from Calbiochem. Anti–HIF-1α antibody was from Novus Biologicals, Inc.; antibodies anti-actin, IκB-α, p-IκB-α (Ser^{32}), c-Src, p65, p50, p52, and MnSOD were from Santa Cruz Biotechnology; whereas antibodies anti–p-c-Src (Tyr^{416}, Tyr^{527}) were from Cell Signaling Technology, Inc. The anti–phosphotyrosine–horseradish peroxidase (HRP)–conjugated antibody was from Zymed. Reporter plasmids pNF-κB-Luc and phRL-TK were from BD Bioscience and Promega, respectively. The hypoxia response element (HRE) luciferase reporter was a generous gift from Dr. A.J. Giaccia (Stanford University, Palo Alto, CA).

Cell culture and incubation. The hepatoblastoma HepG2, H35, and the human neuroblastoma SH-SY5Y cells were obtained from the European Collection of Animal Cell Cultures (Salisbury, Wilts, United Kingdom). SW480 and DLD-1 colon carcinoma cells were a kind gift of Dr. A. Villanueva (IDIBELL, Barcelona, Spain). Cells were cultured in DMEM containing high glucose levels, supplemented with 10% heat-inactivated (56°C, 30 min) fetal bovine serum; 2 mmol/L L-glutamine; 100 units/mL penicillin; 100 μg/mL streptomycin in a humidified atmosphere at 37°C, and 5% CO_2, and 21% O_2 (called normoxic conditions). Hypoxic conditions were attained by exposure to 5% to 2% O_2 and 5% CO_2 in a humidified incubator (Forma Scientific) in sealed flasks for 24 to 72 h as previously described (28). In some cases, hypoxia cells were exposed to inhibitors of mitochondrial electron flow at complexes I/II [rotenone plus TTFA (R/T)] or III (antimycin A), or GSH depletors diethylmaleate and (*R,S*)-3-hydroxy-4-pentenoate (HP). In control experiments, we verified that the instantaneous opening of flasks in the incubator for 10 to 15 s did not result in enhanced ROS stimulation with respect to hypoxic unperturbed flasks (not shown).

Measurement of ROS and cytotoxicity assessment. Hydroethidine (excitation 495 / emission 610) and DCF (excitation 495 / emission 525) fluorescence were determined in a fluorometer at 37°C and the data were normalized to values obtained from normoxic, untreated controls as described before (27, 29). Cytotoxicity was determined by the 3-(4,5-dimethylthiazol-2-yl)-2,5-diphenyltetrazolium bromide (MTT) assay or through the leakage of lactate dehydrogenase into the medium. In some cases, cells were stained with Hoechst 33528 and propidium iodide to examine the extent of apoptotic/necrotic cell death.

Preparation of cytosolic and nuclear extracts. Nuclear and cytosolic extracts of HepG2 and SH-SY5Y cells were prepared by lysing cells with Igepal CA-630 followed by differential centrifugation as before (30, 31).

Electrophoretic mobility shift assay. Activation of transcription factor NF-κB was assessed using consensus oligonucleotides of NF-κB (5′-AGTTGAGGGGACTTTCCCAGGC-3′), with probes labeled as described before (30, 31).

IκB-α immunoprecipitation and immunoblot analysis. HepG2 cells (20×10^6) were treated with 200 μmol/L sodium orthovanadate for 30 min in normoxia or with 10 μmol/L PP2 or 100 μmol/L piceatannol during hypoxia. Cells were lysed with 0.5% Igepal CA-630, 50 mmol/L Tris, 120 mmol/L Tris, 120 mmol/L NaCl (pH 7.8), 1 mmol/L phenylmethylsulfonyl fluoride, 1 mmol/L Na_3VO_4, 10 mmol/L NaF, and incubated for 30 min at 4°C and cell lysates were centrifuged at 14,000 × *g* for 15 min at 4°C. Immunoprecipitation was done using 2 μg IκB-α antibody and 40 μL protein G–agarose beads (Santa Cruz Biotechnology) overnight at 4°C. The precipitates were washed three times in lysis buffer. Membranes were saturated with blocking buffer (5% bovine serum albumin) for 18 h at room temperature and then probed with a mouse anti–phosphotyrosine-HRP–conjugated antibody for 45 min at room temperature. The blots were stained with Ponceau S to confirm the uniformity of protein loading in each lane. Immunodetections were carried out using an enhanced chemiluminescence enhanced chemiluminescence kit (Amersham Biosciences).

RNA isolation and real-time reverse transcription-PCR. Briefly, 20 ng of total RNA, 600 μmol/L of primers, and 12.5 μL of 2× reaction mix were incubated in 25 μL at 50°C for 10 min and 95°C for 5 min, followed by 45 cycles of 95°C for 10 s, 56°C for 30 s, and 72°C for 30 s. Each reaction was run in duplicate and the threshold (C_T) values for each mRNA were subtracted from that of β-actin mRNA, averaged, and converted from log-linear to linear term. The primer sequences used were as follows: *β-actin* forward 5′-TTGCCGACAGGATGCAGAA-3′, reverse 5′-GCCGATCCACACGGAGTACT-3′; *pyruvate dehydrogenase kinase 1* (*PDK1*) forward 5′-GAAGCAGTTCCTGGACTTCG-3′, reverse 5′-ACCAATTGAACGGATGGTGT-3′; *cIAP-2* forward 5′-GTGATGGTGGACTCAGGTGTTG-3′, reverse 5′-TCCTGTCCTTTAATTCTTATCAAGTACTCA-3′; *vascular endothelial growth factor* (*VEGF*) forward 5′-CTACCTCCACCATGCCAAGTG-3′, reverse 5′-TGCGCTGATAGACATCCATGA-3′; and *MnSOD* forward 5′-AACGTCACCGAGGAGAAGTA-3′, reverse 5′-GGCTGAGGTTTGTCCAGAAA-3′.

mGSH depletion. The neuroblastoma cell line SH-SY5Y or the colon carcinoma cell line DLD-1 were preincubated with HP (10 mmol/L, 10 min) to deplete mGSH as described before (27–29). HP undergoes a biotransformation into a Michael electrophile in the matrix, which is then conjugated with GSH.

Cell transfection with reporter constructs. Briefly, 5×10^5 cells were plated onto a 24-well culture plate and transiently transfected using LipofectAMINE 2000 (Invitrogen) with the corresponding reporter plasmid (pNF-κB-Luc or HRE-Luc), the presence or absence of the different c-Src mutants, and phRL-TK for normalization. Cells were harvested 48 to 72 h after transfection, and the Firefly and Renilla luciferase activities were measured with the dual luciferase assay system according to the manufacturer's instructions (Promega).

Site-directed mutagenesis. pSG5 vector–based constructs expressing wild-type Src and its mutants Src C245A and Src C487A were generated as described previously (32), using a QuickChange site-directed mutagenesis kit (Stratagene), confirmed by sequencing, and transfected in HepG2 cells with LipofectAMINE 2000.

Silencing of p65 expression. Specific predesigned small interfering RNAs (siRNA) were ordered to Santa Cruz Biotechnology and transfected in hepatoma cells (HepG2 and H35) with siPORT Amine cationic solution from Ambion according to the manufacturer's instructions. siRNA with equivalent %GC nucleotide content was used as a control. Cells were assayed usually 36 to 72 h after siRNA duplexes transfection. The effect of p65 suppression was monitored by p65 mRNA and protein levels.

Statistical analysis. Results were expressed as the mean ± SD and the statistical significance of the mean values was established by the Student's *t* test.

Results

Hypoxia-induced mROS activate NF-κB and stabilize HIF-1α in HepG2 cells. Hypoxia has been shown to induce an early burst of mROS, which regulate gene expression through activation of transcription factors NF-κB and HIF-1α (16–19), with most studies using severe oxygen deprivation (typically 0.02–1.5%). In the liver, the anatomic structure of this organ determines an O_2 gradient along the acinus as a result of the unidirectional blood flow from the portal vein and hepatic artery to the central vein. The oxygen tension in these populations of hepatocytes ranges from 65 to 60 mm Hg (~10–8% O_2) in the periportal area to 35 to 30 mm Hg (~8–5% O_2) in the perivenous area (34), indicating a hypoxic environment in the latter cell types relative to the former. Because we have recently shown that 5% O_2 increased mROS (28), we analyzed the regulation of NF-κB and HIF-1α in hepatoma cells subjected to 5% O_2 compared with normoxia. The levels of ROS monitored as DCF fluorescence increased at 24 to 72 h after exposure of HepG2 cells to 5% O_2 (Fig. 1*A*), and the magnitude of DCF fluorescence increased further when cells were exposed to 2% O_2 (not shown). Moreover, similar observations were made with the rat hepatoma cell line H35 in which hypoxia-induced DCF fluorescence was lower than in isolated rat hepatocytes (Supplementary Fig. S1). Inhibition of mitochondrial electron flow at complexes I and II with R/T prevented the stimulation of ROS by 5% O_2 (Fig. 1*A*), whereas antimycin A enhanced the generation of ROS caused by 5% O_2, consistent with previous findings (28, 33).

Next, using nuclear extracts prepared at different times during hypoxia, we observed enhanced DNA binding activity of NF-κB that was displaced by an excess of unlabeled κB (Fig. 1*B*). The time-dependent NF-κB activation paralleled that of mROS generation, with no activation observed before 24 h of exposure to 5% O_2 (not shown). Hypoxia activated the p65/p50 and p50/p50 dimers as revealed in supershift assays using specific antibodies (Fig. 1*B*). In addition, a lower molecular weight complex not shifted by any of the antibodies used as well as c-Rel and RelB (not shown) was detected (Fig. 1*B*), although its relevance is uncertain because this complex was not specific for κB (Fig. 1*B*). Moreover, Western blot analyses of nuclear extracts revealed enhanced levels of HIF-1α during hypoxia (Fig. 1*C* and *D*). To assess the contribution of the mROS generation in the activation of NF-κB and HIF-1α stabilization, their regulation was examined in conditions in which mROS generation was modulated. R/T blocked the DNA binding activity of NF-κB and ameliorated the stabilization of HIF-1α caused by hypoxia (Fig. 1*A–C*). Moreover, the transcriptional activity of HIF-1α and NF-κB during 5% O_2 was examined using a HRE-luciferase reporter and by real-time PCR. Hypoxia enhanced the luciferase activity in HepG2 cells transfected with the reported construct (Fig. 2*A*). Moreover, the mRNA levels of HIF-1α and NF-κB target genes such as *VEGF, PDK1*, and the antiapoptotic protein cIAP-2, respectively, increased by hypoxia (Fig. 2*A*). Moreover, R/T treatment prevented hypoxia-induced VEGF, PDK1, and cIAP-2 mRNA levels, whereas antimycin A did not (Fig. 2*A*). Together, these findings validate the involvement of mROS generation in the activation of NF-κB and HIF-1α stabilization by hypoxia.

Hypoxia activates NF-κB without IκB-α degradation via IκB-α tyrosine phosphorylation. As outlined above, the mechanism of NF-κB activation by hypoxia has not been well established, particularly in the light of the different fate of IκB-α after phosphorylation at serine or tyrosine residues that determine the degradation or not, respectively, of IκB-α by the proteasome (21–23, 25, 35). Thus, we examined the phosphorylation state of IκB-α during hypoxia in hepatoma cells. In contrast to prior observations in Jurkat T-cells subjected to very low oxygen concentrations (24), the levels of IκB-α remained constant during 5% O_2 exposure, similar to the levels of normoxic cells (Fig. 2*B*), and this outcome resulted in enhanced NF-κB DNA binding (Fig. 1*B*). To further validate this finding, HepG2 cells were exposed to TNF, a cytokine that activates NF-κB by the proteasome-mediated degradation of IκB-α secondary to its phosphorylation in serine 32. Unlike hypoxia, TNF (100 units/mL for 30 min) decreased the levels of IκB-α (Fig. 2*B*), and this outcome was accompanied by p65/p50– and p50/p50–enhanced DNA binding (not shown). Moreover, in conditions in which the proteasome was inhibited by *N*-acetyl-leucyl-leucyl-norleucinal, TNF induced the phosphorylation of IκB-α at Ser^{32}, whereas hypoxia did not (Fig. 2*B*). To monitor if IκB-α was phosphorylated in tyrosine residues, IκB-α was immunoprecipitated and probed with anti-phosphotyrosine antibodies. As seen, hypoxia increased the phosphorylation of IκB-α in tyrosine residues (Fig. 2*C*), with similar results observed upon pervanadate exposure (Supplementary Fig. S2), in agreement with previous reports (23, 35). Taken together, these findings indicate that hypoxia per se activates NF-κB via tyrosine IκB-α phosphorylation in the absence of IκB-α degradation.

Critical role of Cys^{487} in hypoxia-induced c-Src activation. Next, we examined the involvement of specific tyrosine kinases that may have contributed to the tyrosine phosphorylation of IκB-α during hypoxia. We focused on c-Src, a 60-kDa prototypical Src family member that plays an important role in cell cycle control, adhesion, and oncogenesis, because previous observations in HeLa cells implicated this particular kinase in the tyrosine phosphorylation of IκB-α after hypoxia/reoxygenation (26). We first examined the activation of c-Src after exposure to 5% O_2. Compared with normoxia, the level of c-Src did not change during the time course of hypoxia. However, the phosphorylation of c-Src in Tyr^{416} increased during hypoxia, whereas that of Tyr^{527} did not (Fig. 2*D*). Furthermore, consistent with the inhibitory effect of R/T on mROS generation and NF-κB activation (Fig. 1*A* and *B*), these mitochondrial inhibitors prevented the phosphorylation of c-Src at Tyr^{416}, whereas antimycin A, which potentiated mROS (Fig. 1*A*), enhanced the levels of c-Src Tyr^{416} phosphorylation (Fig. 2*D*). The functional link between mROS generation by hypoxia and the subsequent activation of c-Src was further studied using oxidant insensitive c-Src mutants. Although five cysteine residues, Cys^{238}, Cys^{245}, Cys^{400}, Cys^{487}, and Cys^{498}, are conserved among all c-Src family members, the mutants C245A and C487A in which the Cys^{245} of the SH2 domain and Cys^{487} of the kinase domain, respectively, were replaced by alanine residues were chosen as these mutants were reported to play a critical role in adhesion-dependent c-Src activation (32). Hypoxia stimulated Src Tyr^{416} phosphorylation in C245A mutants, but not in C487A mutants (Fig. 2*D*), indicating a critical role for Cys^{487} in c-Src activation by hypoxia.

mROS-induced c-Src stimulation activates NF-κB. Next, we determined the role of c-Src in NF-κB activation by examining the effect of PP2, a c-Src tyrosine kinase inhibitor, versus piceatannol that selectively inhibits ZAP-70/Syk kinase (35–37). PP2 blocked the activation of c-Src monitored as the phosphorylation of Tyr^{416} (Fig. 2*D*) and prevented the tyrosine phosphorylation of IκB-α (Fig. 2*C*), the subsequent DNA binding activity of NF-κB (Fig. 3*A*),

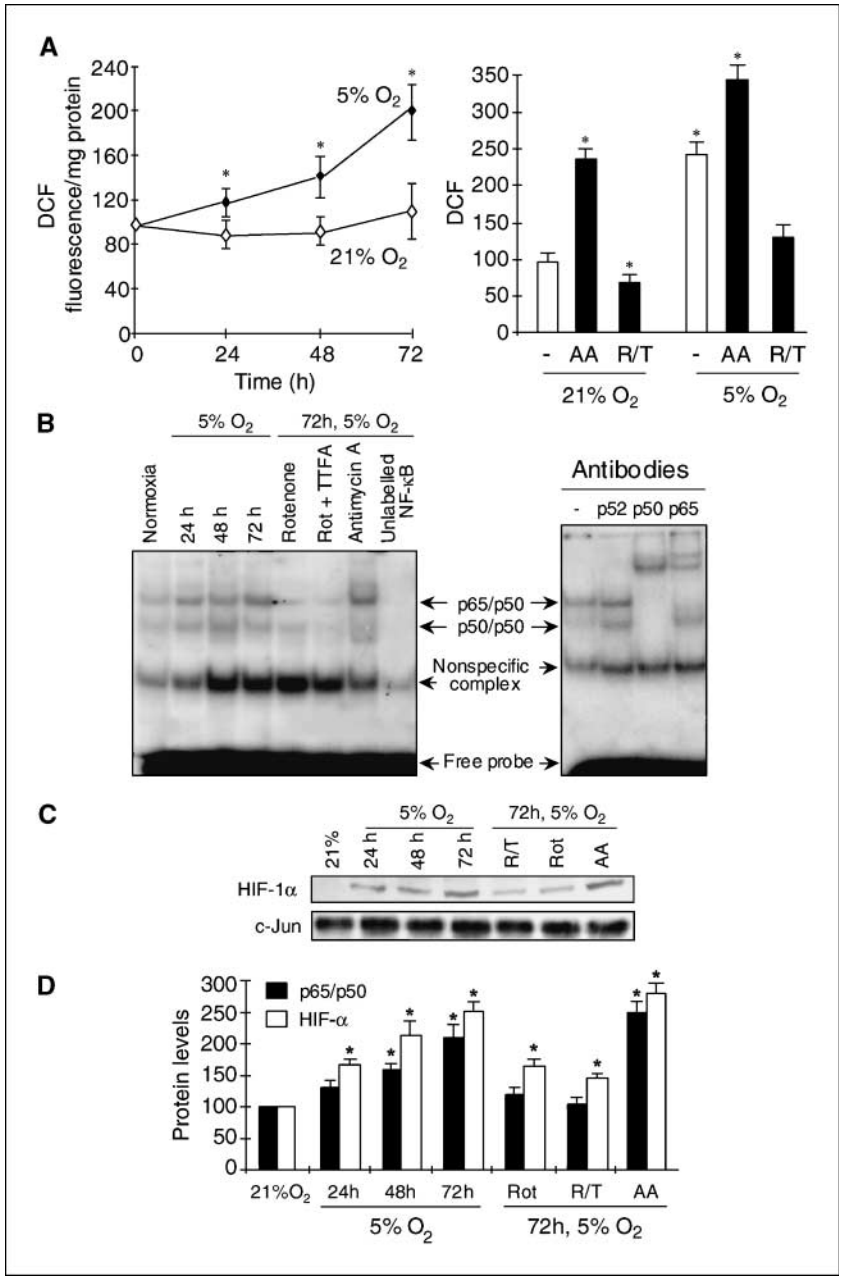

Figure 1. Hypoxia-induced mROS activate transcription factor HIF-1α and NF-κB. *A,* HepG2 cells were cultured under 5% O_2 or 21% O_2 for various periods to determine DCF fluorescence. In some cases, cells were incubated in the presence of 2.5 μmol/L rotenone plus 2 μmol/L TTFA (*R/T*) or 10 μmol/L antimycin A (*AA*) for the last 6 h of the 72-h period in normoxic or hypoxic conditions (5% O_2). ROS generation was measured after DCF fluorescence. *B,* nuclear extracts were isolated and processed for the activation of NF-κB by electrophoretic mobility shift assay shown in the representative image, with or without incubation with R/T or antimycin A. Four separate experiments were done with similar results. In some cases, anti-p52, anti-p50, or anti-p65 antibody was included before the electrophoretic mobility shift assay. *C,* nuclear extracts were immunoblotted with anti–HIF-1α antibody to determine the levels of this transcription factor during hypoxia with or without incubation with R/T or antimycin A. *D,* the levels of the heterodimer p65/p50 or HIF-1α shown in (*B*) and (*C*) were quantitated by densitometry ($n = 4–5$). *, $P < 0.05$ versus normoxia.

and the c-IAP2 expression by hypoxia (Fig. 2*A*). In contrast, the tyrosine phosphorylation of IκB-α (Fig. 2*C*) and the NF-κB activation by hypoxia still occurred in the presence of piceatannol (Fig. 3*A*), discarding a role for ZAP-70 and Syk Src family members in the activation of NF-κB by hypoxia. To further validate the role of c-Src, we examined the effect of C245A and C487A c-Src mutants in the activation of NF-κB by hypoxia using the reporter plasmid pNF-κB-Luc. The activation of NF-κB occurred both in wild-type c-Src and C245A mutants and this outcome was ameliorated in C487A mutants-expressing cells (Fig. 3*B*), consistent with the findings on the critical role of Cys^{487} in c-Src activation by hypoxia. In contrast, neither PP2 nor the transfection of the c-Src constructs prevented the activation of HIF-α induced by hypoxia (Supplementary Fig. S3). These findings establish a functional link between the c-Src and NF-κB during hypoxia.

NF-κB down-regulation or c-Src inhibition sensitizes hepatoma cells to hypoxia. Given the critical role of NF-κB in cell survival, we next examined the effect of NF-κB down-regulation on the cellular susceptibility to hypoxia. The p65 member of NF-κB in HepG2 cells was targeted by siRNA, examining the survival during exposure to 5% O_2. Transfection of cells with p65 siRNA significantly reduced the mRNA levels of p65 compared with cells transfected with a scrambled control siRNA (Fig. 3*C*). Furthermore, p65 siRNA reduced the levels of p65 in nuclear extracts after hypoxia exposure compared with cells transfected with scrambled control siRNA (Fig. 3*C*). Moreover, although cells transfected with the control siRNA were resistant to 5% O_2, as expected based on previous findings (38), HepG2 cells transfected with p65 siRNA exhibited a significant susceptibility to hypoxia-induced cell death (Fig. 3*D*). Similar results were observed with H35 hepatoma cells

(not shown). Furthermore, consistent with the upstream role of c-Src in the activation of NF-κB, PP2 that prevented the NF-κB activation (Fig. 3*A*) sensitized HepG2 cells to hypoxia although to a lesser extent than that observed upon p65 down-regulation (Fig. 3*D*). To further analyze the potential mechanism underlying the susceptibility to hypoxia after NF-κB down-regulation, we focused on the regulation of MnSOD, a known κB-controlled antioxidant enzyme. As seen, MnSOD expression was reduced upon p65 down-regulation by siRNA (Fig. 3*C*), translating in a significant overgeneration of mROS by 5% O_2 (Fig. 3*D*). However, MnTBAP, a cell-permeable porphyrin SOD mimetic, reduced mROS generation and protected HepG2 cells against 5% O_2 after p65 siRNA exposure (Fig. 3*D*). Hence, these findings indicate that the c-Src–NF-κB signaling protects hepatoma cells during hypoxia, in part, through the κB-regulated MnSOD.

mGSH depletion sensitizes cancer cells to hypoxia without disabling the c-Src-NF-κB signaling. Because mGSH regulates mROS generation (39), we addressed whether mROS overgeneration by mGSH depletion sensitizes cancer cells to hypoxia. mGSH depletion can be achieved *in vitro* in a selective fashion by incubation of cells with HP, which is biotransformed in mitochondria into a Michael electrophile, being conjugated with matrix GSH with the sparing of cytosolic GSH (27–29, 40). Human neuroblastoma SH-SY5Y cells were treated with HP, examining the compartmentation of GSH into the cytosol and mitochondria. HP led to a selective depletion of mGSH by 60% to 70% without effect on the cytosol pool of GSH (Fig. 4*A*). Because most studies used low oxygen concentrations (up to 1.5–2%), we examined the effect of HP in the susceptibility to 2% O_2. HP treatment enhanced hypoxia-induced ROS generation in SH-SY5Y (Fig. 4*A*) that translated in a significant loss of cell viability (Fig. 4*B*). Staining cells with Hoechst 33258 and propidium iodide indicated a predominant population of propidium iodide–positive cells with minimal altered chromatin morphology (Fig. 4*C*). Similar findings in terms of ROS production and survival after HP treatment were observed during the exposure of cells to 5% O_2 (Supplementary Fig. S4). Furthermore, HP selectively depleted mGSH in colon carcinoma DLD-1 cells, resulting in their sensitization to hypoxia-induced cell death (Fig. 4*D*). The susceptibility to hypoxia by HP in SH-SY5Y and DLD-1 cells was prevented by the antioxidant butylated hydroxytoluene or incubation with GSH-ethyl ester (not shown). Unlike SH-SY5Y and DLD-1 cells, several hepatoma cells tested, including HepG2, Hep3B, H35, or Hepa1c1c7, failed to respond to the selective mGSH depletion by HP (not shown), due to the inability to these cells to generate the 3-oxo-4-pentenoate derivative from HP within the mitochondria (41). In addition, the selective decrease of the cytosolic GSH levels by diethylmaleate (0.2 mmol/L) was not effective in inducing cell death by hypoxia nor did it increase mROS production (Supplementary Figs. S5 and S6), thus underscoring the importance of the mitochondrial pool of GSH rather than cytosol GSH in the regulation of mROS and protection against hypoxia.

Furthermore, because ROS plays a bifunctional role in the regulation of NF-κB, we examined the relationship of the mGSH depletion–mediated susceptibility to hypoxia with the c-Src–NF-κB pathway. Kinetic analyses of $pTyr^{416}$ c-Src phosphorylation and p65 levels in nuclear extracts revealed that HP pretreatment neither prevented the activation of c-Src and NF-κB caused by hypoxia (Fig. 5*A*) nor changed the activation of HIF-1α measured using an HRE reporter vector (Supplementary Fig. S3). However, HP treatment did result in an accelerated and enhanced burst of

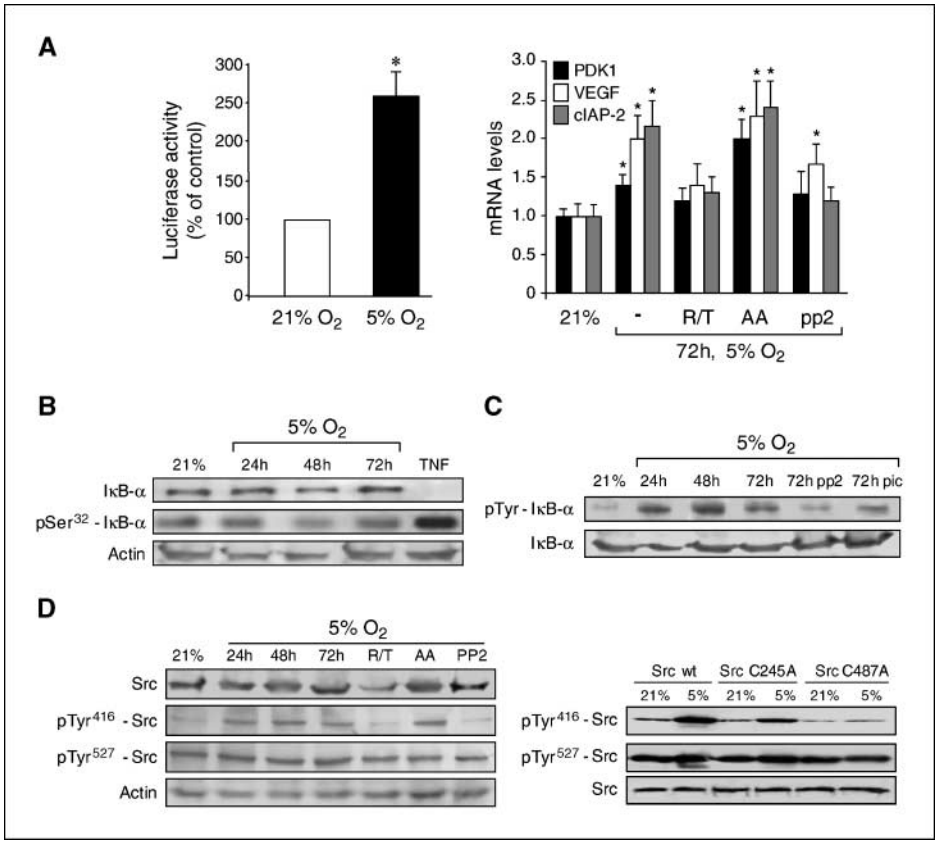

Figure 2. HIF-1α and NF-κB activation and expression of target genes during hypoxia. *A,* HepG2 cells were transfected with the HRE luciferase reporter construct and subjected to hypoxia for 72 h ($n = 3$). *, $P < 0.05$ versus normoxia. The mRNA levels of PFK1, VEGD, and cIAP-2 from HepG2 cells subjected to hypoxia were determined by real-time PCR with or without incubation with R/T, antimycin A, or PP2 ($n = 4$–5). *, $P < 0.05$ versus normoxia. *B,* the levels of IκB-α and phospho-Ser^{32} IκB-α were determined in cell extracts from HepG2 cells subjected to hypoxia and compared with those obtained after incubation with TNF (100 units/mL). A representative blot out of four experiments exhibiting similar results. *C,* the levels of phospho–Tyr-IκB-α in cell extracts from HepG2 cells subjected to hypoxia with or without PP2 or picceatanol (*pic*). Representative blot ($n = 4$). *D,* the levels of Src and phospho-Src in Tyr^{416} and Tyr^{527} with or without the effect of R/TTFA, antimycin A, or PP2 ($n = 4$). In some cases, HepG2 cells were transfected with wild-type Src, C245A, and C487A Src mutants and then subjected to hypoxia (5% O_2) for 72 h to monitor the levels of phospho-Tyr^{416} and phospho-Tyr^{527}. One blot out of three independent experiments with similar results.

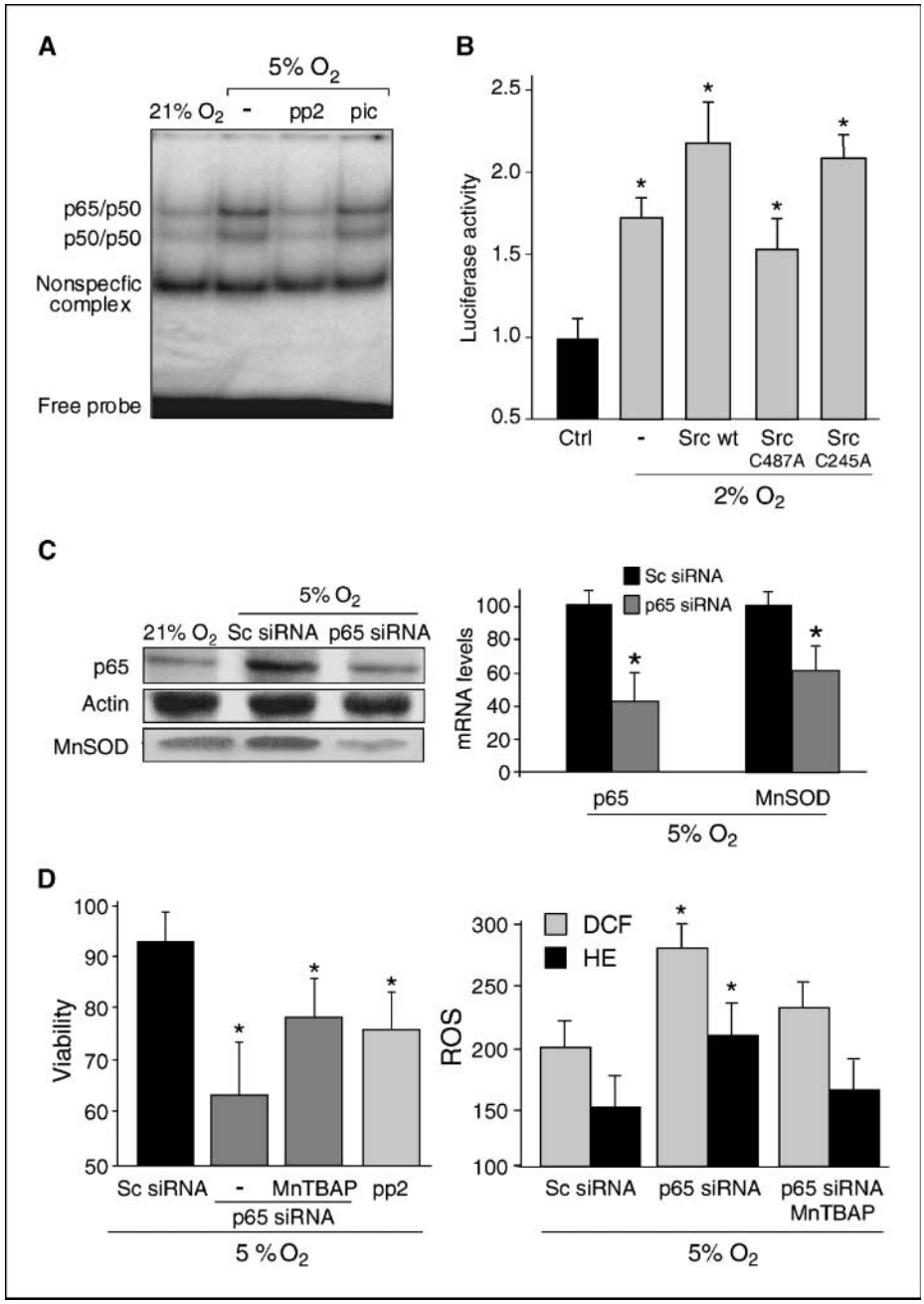

Figure 3. NF-κB down-regulation sensitizes HepG2 cells to hypoxia. *A,* HepG2 cells were subjected to hypoxia for 72 h and then nuclear extracts were examined for NF-κB activation by electrophoretic mobility shift assay in the presence or absence of PP2 or picceatanol. *B,* in some cases, HepG2 cells were transfected with a NF-κB luciferase reporter construct and redox-insensitive Src mutants and subjected to hypoxia for 72 h ($n = 3$). *, $P < 0.05$ versus normoxia. *C,* HepG2 cells were transfected with control siRNA or siRNA targeting p65 and the protein and mRNA levels for p65 and MnSOD during hypoxia for 72 h were analyzed by Western blot and real-time PCR, respectively ($n = 3$). *D,* the survival of HepG2 that have been transfected with control siRNA (*Sc siRNA*), or siRNA targeting p65 in the presence or absence of the SOD mimetic MnTBAP (50 μmol/L), or incubated with PP2 to inhibit Src was examined after 3 d of hypoxia ($n = 3$–6). *, $P < 0.05$ versus normoxia. In some cases, ROS generation was measured by adding the fluorescent probes hydroethidine (*HE*; 5 μmol/L) and DCF (1 μmol/L) to the cells during 30 min at 37°C ($n = 3$). *$P < 0.05$ versus normoxia.

mROS by hypoxia (Fig. 5*B*), and this enhanced ROS formation mirrored the temporal reduction of cell viability during hypoxia (Fig. 5*C*). Moreover, consistent with these findings, HP potentiated the release of Smac/DIABLO and cytochrome *c* during hypoxia (Fig. 5*D*) and mitochondrial membrane depolarization (not shown). These findings establish a critical role for mROS in the susceptibility to hypoxia.

Discussion

The present study addressed the role of mROS in the survival/susceptibility of cancer cells during hypoxia. Hypoxia is a prominent feature of solid tumor development considered a major driving force for tumor progression. Indeed, the higher malignancy of hypoxic tumors has been attributed to the ability of hypoxia to select for cells that are resistant to cell death and to the increase in tumor cell invasiveness (1–3, 42). Thus, strategies that sensitize cancer cells to hypoxia may be of therapeutic relevance.

Our findings highlight a dual role of mROS in hypoxia signaling (Fig. 6). The generation of ROS during hypoxia, and their role in oxygen sensing, has been a controversial issue (6, 14, 15). However, recent compelling evidence using genetic and biochemical approaches indicated a burst of mROS at mitochondrial complex III. Although the exact mechanisms involved are currently unknown, mROS generation by hypoxia stabilize HIF-1α with the Rieske iron-sulfur protein-mediated superoxide anion generation playing a crucial role (16–18). The regulation of PHDs by oxidant signals is poorly understood, and the mechanism of mROS-mediated PHD

inhibition underlying the reported HIF-1α stabilization remains to be established. Nevertheless, mROS can inhibit PHDs as a result of ROS-mediated depletion of ascorbate, which could limit the regeneration of Fe (II) from Fe (III) needed for PHD activity. Moreover, despite the role for oxidant-dependent HIF-1α stabilization, there is also evidence for the regulation of HIF-1α independently of ROS. For instance, recent findings have indicated that accumulation of succinate in normoxia due to the deletion of succinate dehydrogenase induced the HIF-1α transcriptional activity through inhibition of PHD (43). Consistent with this conception, we observed that R/T ameliorated the stabilization of HIF-1α although it efficiently prevented the mROS burst generated by hypoxia.

We established a functional link between the mROS production and the activation of NF-κB through c-Src stimulation (Fig. 6). Although the activation of NF-κB by hypoxia has been described, the mechanism involved was poorly characterized with a number of inconsistencies regarding the differential fate of IκB-α after phosphorylation in serine or tyrosine residues (23–25). Our data indicate that the early burst of mROS links c-Src with NF-κB activation through tyrosine IκB-α phosphorylation, as R/T, which prevents mROS generation, blocks the appearance of a Tyr^{416} phosphorylated form of c-Src, indicating a role for superoxide anion generation in this event. Due to the reactivity of superoxide anion and its expected low diffusion from mitochondria, it is likely that its conversion into hydrogen peroxide and diffusion into cytosol may target the redox-sensitive c-Src Cys^{487}. Our findings linking mROS with c-Src are consistent with those observed in vascular smooth muscle cells cultured under an oxygen tension of <1 mm Hg, as rotenone and DPI abolished the mitochondrial ROS

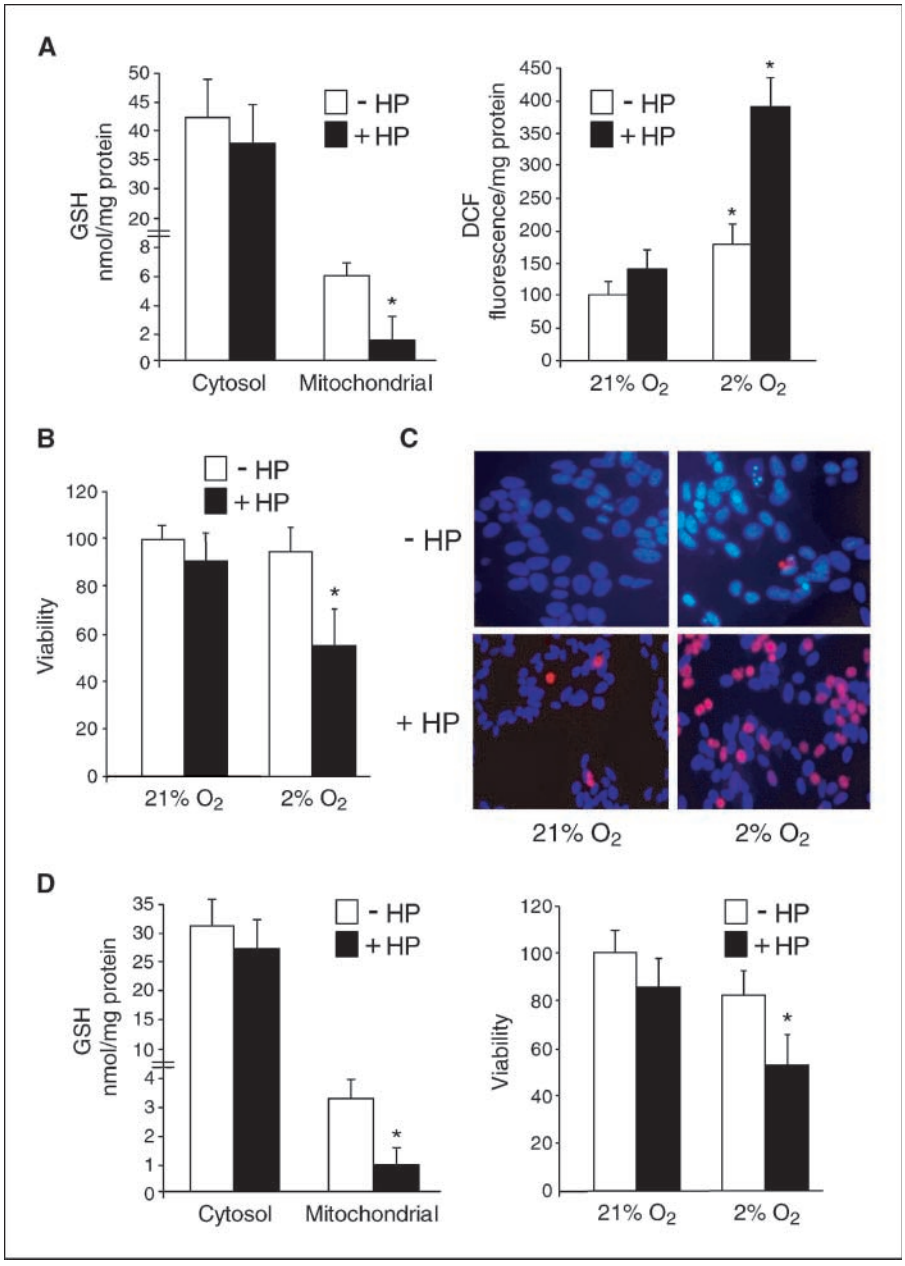

Figure 4. Selective mGSH depletion sensitizes SH-SY5Y and DLD-1 cancer cells to hypoxia. *A,* SH-SY5Y cells were incubated with HP and then fractionated into cytosol and mitochondria to determine GSH levels ($n = 4$). Afterward, cells were subjected to hypoxia for 48 h to measure ROS generation by DCF fluorescence. *, $P < 0.05$ versus cells without HP. *B,* the effect of HP on the survival was examined during hypoxia for 48 h ($n = 4$). *, $P < 0.05$ versus cells without HP. *C,* microscopic images of SH-SY5Y cells stained with propidium iodide and Hoechst 33528. *D,* colon carcinoma cells DLD-1 were incubated with HP and the compartmentation of GSH in cytosol and mitochondria analyzed. The survival of DLD-1 cells during hypoxia after HP exposure was analyzed by MTT assay ($n = 3$). *, $P < 0.05$ versus normoxia.

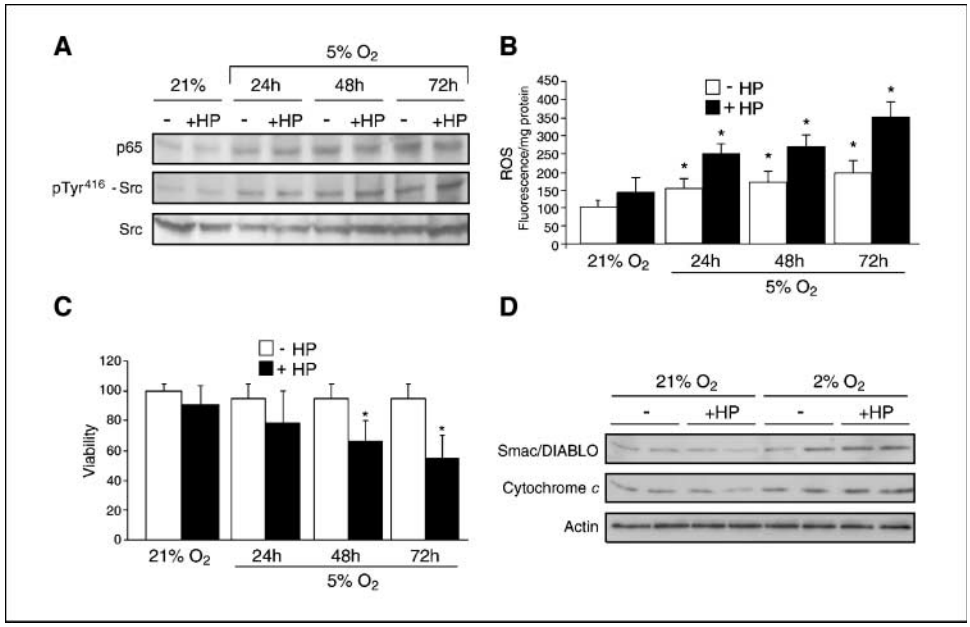

Figure 5. Kinetics of p65, phospho-Tyr^{416} Src, and survival of SH-SY5Y cells during hypoxia after HP exposure. *A,* SH-SY5Y cells were preincubated with HP and then subjected to hypoxia for the indicated period of time to analyze the levels of p65 in nuclear extracts and phospho-Tyr^{416} Src in cells extracts. A representative blot out of three independent experiments with similar results. *B* and *C,* DCF fluorescence and survival, respectively, were examined at various times during hypoxia after HP preincubation or without HP incubation (n = 3–4). *, $P < 0.05$ versus cells without HP incubation. *D,* SH-SY5Y cells were subjected to hypoxia for 48 h with or without HP incubation to analyze the release of Smac/DIABLO and cytochrome *c* release from mitochondria. Representative blot (n = 3).

generation and c-Src activation induced by hypoxia (44). Furthermore, recent observations reported the recruitment of c-Src to mitochondria by Dok-4, a downstream of kinase family of adapter proteins, resulting in mitochondrial complex I down-regulation, ROS generation, and NF-κB activation by TNF (45). Whether the putative trafficking of c-Src to mitochondria played a role in hypoxia-induced c-Src activation remains to be established. Although we observe that cells are resistant to 5% O_2, as previously reported (38), NF-κB appears to modulate the susceptibility of hepatoma cells to hypoxia, in agreement with previous observations in ventricular myocytes (46), possibly due to the regulation of mROS generation via MnSOD, although other factors such as the repression of the death gene *BNIP3* by NF-κB may also play a role.

Given the key role of HIF-1α stabilization and NF-κB activation in promoting survival of cancer cells, angiogenesis, neovascularization, glycolytic ATP generation, and tumor invasion (1, 2, 10), and

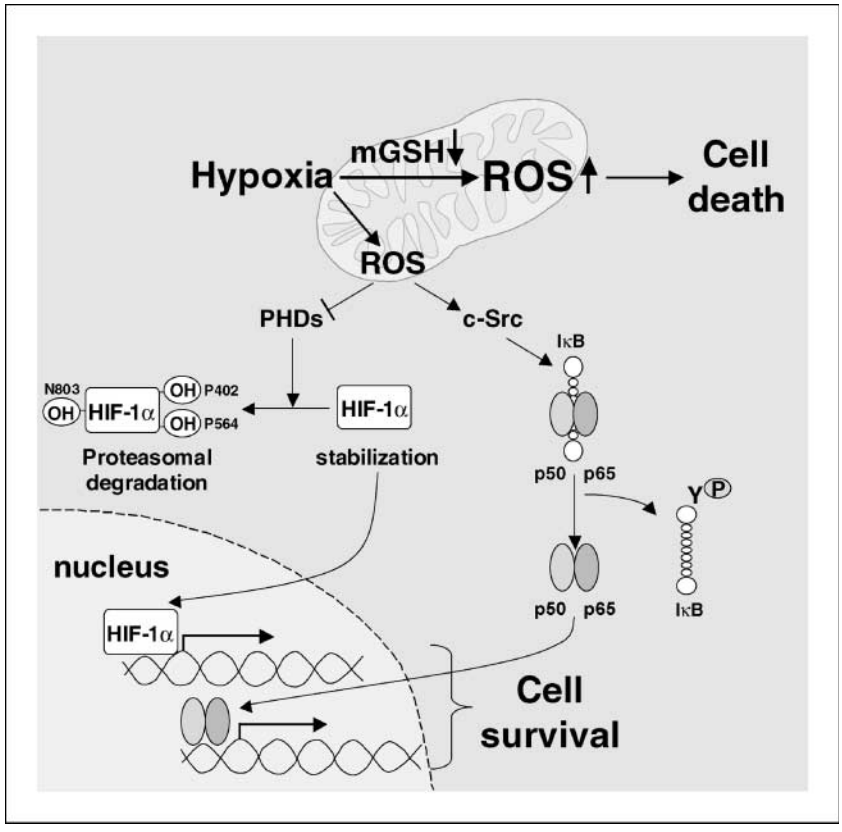

Figure 6. Dual role of mROS in hypoxia signaling. Hypoxia generates mROS, which, in turn, activate NF-κB through c-Src–mediated phosphorylation of IκB-α at tyrosine residues, and the stabilization of HIF-1α. These events promote carcinogenesis through maintenance of cell survival and tumor progression. However, when mGSH is depleted, hypoxia induces an enhanced formation of mROS stimulating the release of cytochrome *c*, resulting in oxidant-dependent cell death.

consistent with the view that ROS promote carcinogenesis (47), our findings suggest that hypoxia-induced mROS act as procarcinogenic signals. In addition, cancer cells exhibit greater ROS generation determining an intrinsic oxidative stress that could contribute to their vulnerability to free radical–induced cell death. Consistent with this view, we observe that mROS overgeneration due to mGSH depletion determines the susceptibility of cancer cells to hypoxia, suggesting that this strategy may be of relevance to turn the hypoxic environment of solid tumors into a therapeutic milieu to kill cancer cells. Interestingly, although we observed the mitochondrial release of apoptotic factors, most of the cells dying during hypoxia after mGSH depletion exhibit necrotic features possibly due to the overgeneration of mROS under these conditions. In this regard, a dual role for oxidants and ROS in the regulation of caspase activity has been described, implying that excess ROS inhibit caspases favoring the necrotic demise of cells (48). Despite that the selective depletion of mGSH by HP is cell type specific, strategies that result in total cell GSH depletion (cytosol and mitochondrial pools) may be also useful to kill cancer cells, as the mitochondrial GSH pool derives from the cytosol GSH pool (39). In this regard, recent observations reported the killing of oncogenically transformed cells through a ROS-mediated mechanism by β-phenylethyl isothiocyanate (PEITC), which depletes total GSH levels, although the regulation of mGSH was not examined (49). Moreover, we have shown that diethylmaleate and buthionine-L-sulfoximine, which deplete GSH levels both in cytosol and mitochondria, sensitized HepG2 cells to 5% O_2–induced cell death, which was prevented by R/T despite profound cytosol GSH depletion (28). Unlike total GSH depletion, which blocks redox-dependent signals such as NF-κB as reported with PEITC (49), the selective mGSH depletion by HP did not interfere with hypoxia-induced NF-κB activation or c-Src stimulation, and similar findings in this regard have been recently reported with TNF (29). Therefore, our observations along with prior reports describing that enhanced ROS generation by blocking mitochondrial respiration effectively kills human leukemia cells (50) highlight the potential of mROS regulation in cancer therapy.

A caveat from our findings is that HP-mediated sensitization to hypoxia is not specific for cancer cells (27–29). However, mGSH depletion per se is not cytotoxic to normal or cancer cells, although this outcome synergizes with hypoxia to overgenerate cytotoxic amounts of mROS. Moreover, although a systematic comparison in the susceptibility of cancer cells to hypoxia compared with their normal counterparts is not always possible, it is known that hepatoma cells are more resistant to hypoxia than primary hepatocytes (28). Although the reason for this is unclear, many tumor cells, including hepatoma cells, generate less mROS in response to hypoxia than primary cells (28), by a mechanism related to a lower respiratory rate and oxidative phosphorylation, consistent with their dependency on glycolysis for energy production. Thus, although the pharmacologic depletion of mGSH may occur in cancer and healthy cells after HP or other strategies that cause total GSH loss, hypoxia is expected to predominantly affect cancer cells from solid tumors, and hence the combination of mGSH depletion and hypoxia may be of relevance in cancer therapy.

Acknowledgments

Received 2/6/2007; revised 4/26/2007; accepted 5/23/2007.

Grant support: Research Center for Liver and Pancreatic Diseases grant P50-AA11999 funded by the National Institute on Alcohol Abuse and Alcoholism; Plan Nacional de I+D Grant SAF 2006-6780; Fondo de Investigaciones Sanitarias, FISS 06/0495 and FISS 03/0426; and CIBEREHD supported by Instituto de Salud Carlos III. J.M. Lluis and A. Morales are Juan de la Cierva and Ramon y Cajal Investigators, respectively.

The costs of publication of this article were defrayed in part by the payment of page charges. This article must therefore be hereby marked *advertisement* in accordance with 18 U.S.C. Section 1734 solely to indicate this fact.

We thank Susana Nuñez for technical assistance.

References

1. Giaccia A, Siim BG, Johnson RS. HIF-1 as a target for drug development. Nat Rev Drug Discov 2003;2:803–11.
2. Semenza GL. Targeting HIF-1 for cancer therapy. Nat Rev Cancer 2003;3:721–32.
3. Melillo G. Inhibiting hypoxia-inducible factor 1 for cancer therapy. Mol Cancer Res 2006;4:601–5.
4. Pugh CW, Ratcliffe PJ. Regulation of angiogenesis by hypoxia: role of the HIF system. Nat Med 2003;9:677–84.
5. Safran M, Kaelin WG, Jr. HIF hydroxylation and the mammalian oxygen-sensing pathway. J Clin Invest 2003;111:779–83.
6. Kaelin WG, Jr. ROS: really involved in oxygen sensing. Cell Metab 2005;1:357–8.
7. Kallio PJ, Wilson WJ, O'Brien S, Makino Y, Poellinger L. Regulation of the hypoxia-inducible transcription factor 1α by the ubiquitin-proteasome pathway. J Biol Chem 1999;274:6519–25.
8. Hewitson, KS, McNeill LA, Riordan MV, et al. Hypoxia-inducible factor (HIF) asparagine hydroxylase is identical to factor inhibiting HIF (FIH) and is related to the cupin structural family. J Biol Chem 2002;277:26351–5.
9. Lando D, Peet DJ, Gorman JJ, Whelan DA, Whitelaw ML, Bruick RK. FIH-1 is an asparaginyl hydroxylase enzyme that regulates the transcriptional activity of hypoxia-inducible factor. Genes Dev 2002;16:1466–71.
10. Berra E, Ginouves A, Pouyssegur J. The hypoxia-inducible-factor hydroxylases bring fresh air into hypoxia signalling. EMBO Rep 2006;7:41–5.
11. Maxwell PH, Wiesener MS, Chang GW, et al. The tumour suppressor protein VHL targets hypoxia-inducible factors for oxygen-dependent proteolysis. Nature 1999;399:271–5.
12. Kamura T, Sato S, Iwai K, Czyzyk-Krzeska M, Conaway RC, Conaway JW. Activation of HIF1 ubiquitination by a reconstituted von Hippel-Lindau (VHL) tumor suppressor complex. Proc Natl Acad Sci U S A 2000;97:10430–5.
13. Hirsila M, Koivunen P, Gunzler V, Kivirikko KI, Myllyharju J. Characterization of the human prolyl 4-hydroxylases that modify the hypoxia-inducible factor. J Biol Chem 2003;278:30772–80.
14. Vaux EC, Metzen E, Yeates KM, Ratcliffe PJ. Regulation of hypoxia-inducible factor is preserved in the absence of a functioning mitochondrial respiratory chain. Blood 2001;98:296–302.
15. Srinivas V, Leshchinsky L, Sang N, King MP, Minchenko A, Caro J. Oxygen sensing and HIF-1 activation does not require an active mitochondrial respiratory chain electron-transfer pathway. J Biol Chem 2001;276:21995–2002.
16. Brunelle JK, Bell EL, Quesada NM, et al. Oxygen sensing requires mitochondrial ROS but not oxidative phosphorylation. Cell Metab 2005;1:409–14.
17. Guzy RD, Hoyos B, Robin E, Chen H, Liu L, Mansfield KD. Mitochondrial complex III is required for hypoxia-induced ROS production and cellular oxygen sensing. Cell Metab 2005;1:401–8.
18. Mansfield KD, Guzy RD, Pan Y, et al. Mitochondrial dysfunction resulting from loss of cytochrome *c* impairs cellular oxygen sensing and hypoxic HIF-α activation. Cell Metab 2005;1:393–9.
19. Chandel NS, Trzyna WC, McClintock DS, Schumacker PT. Role of oxidants in NF-κB activation and TNF-α gene transcription induced by hypoxia and endotoxin. J Immunol 2000;165:1013–21.
20. Brown K, Gerstberger S, Carlson L, Franzoso G, Siebenlist U. Control of IκB-α proteolysis by site-specific, signal-induced phosphorylation. Science 1995;267:1485–8.
21. Traenckner EB, Pahl HL, Henkel T, Schmidt KN, Wilk S, Baeuerle PA. Phosphorylation of human IκB-α on serines 32 and 36 controls IκB-α proteolysis and NF-κB activation in response to diverse stimuli. EMBO J 1995;14:2876–83.
22. Baeuerle PA, Baltimore D. IκB: a specific inhibitor of the NF-κB transcription factor. Science 1998;242:540–8.
23. Imbert V, Rupec RA, Livolsi A, et al. Tyrosine phosphorylation of IκB-α activates NF-κB without proteolytic degradation of IκB-α. Cell 1996;86:787–98.
24. Koong AC, Chen EY, Giaccia AJ. Hypoxia causes the activation of nuclear factor κB through the phosphorylation of IκBα on tyrosine residues. Cancer Res 1994;54:1425–30.
25. Zwaka R, Zhang Y, Zhou W, Halldorson J, Engelhardt JE. Ischemia/reperfusion injury in the liver of BALB/c mice activates AP-1 and nuclear factor κB independently of IkB degradation. Hepatology 1998;28:1022–30.
26. Fan C, Li Q, Ross D, Engelhardt JF. Tyrosine phosphorylation of IκBα activates NFκB through a redox-regulated and c-Src-dependent mechanism following hypoxia/reoxygenation. J Biol Chem 2003;278:2072–80.
27. Garcia-Ruiz C, Colell A, Mari M, et al. Defective TNF-α-mediated hepatocellular apoptosis and liver damage in acidic sphingomyelinase knockout mice. J Clin Invest 2003;111:197–208.
28. Lluis JM, Morales A, Blasco C, et al. Critical role of mitochondrial glutathione in the survival of hepatocytes during hypoxia. J Biol Chem 2005;280:3224–32.
29. Mari M, Caballero F, Colell A, et al. Mitochondrial

free cholesterol loading sensitizes to TNF and Fas mediated steatohepatitis. Cell Metab 2006;4:185–98.
30. Roman J, Colell A, Blasco C, et al. Differential role of ethanol and acetaldehyde in the induction of oxidative stress in HEP G2 cells: effect on transcription factors AP-1 and NF-κB. Hepatology 1999;30:1473–80.
31. Roman J, Gimenez A, Lluis JM, et al. Enhanced DNA binding and activation of transcription factors NF-κB and AP-1 by acetaldehyde in HEPG2 cells. J Biol Chem 2000;275:14684–90.
32. Giannoni E, Buricchi F, Raugei G, Ramponi G, Chiarugi P. Intracellular reactive oxygen species activate Src tyrosine kinase during cell adhesion and anchorage-dependent cell growth. Mol Cell Biol 2005;25:6391–403.
33. Chandel NS, Maltepe E, Goldwasser E, Mathieu CE, Simon MC, Schumacker PT. Mitochondrial reactive oxygen species trigger hypoxia-induced transcription. Proc Natl Acad Sci U S A 1998;95:11715–20.
34. Jungermann K, Kietzmann T. Zonation of parenchymal and nonparenchymal metabolism in liver. Annu Rev Nutr 1996;16:179–203.
35. Livolsi A, Busuttil V, Imbert V, Abraham RT, Peyron JF. Tyrosine phosphorylation-dependent activation of NF-κB. Requirement for p56 LCK and ZAP-70 protein tyrosine kinases. Eur J Biochem 2001;268:1508–15.
36. Hanke J, Gardner J, Dow R, et al. Discovery of a novel, potent, and Src family-selective tyrosine kinase inhibitor. Study of Lck- and Fyn T-dependent T cell activation. J Biol Chem 1996;271:695–701.
37. Oliver J, Burg D, Wilson B, McLaoughlin J, Gaehlen R. Inhibition of mast cell Fc epsilon R1-mediated signaling and effector function by the Syk-selective inhibitor, piceatannol. J Biol Chem 1994;269:29697–703.
38. Graeber TG, Osmanian C, Jacks T, et al. Hypoxia-mediated selection of cells with diminished apoptotic potential in solid tumors. Nature 1996;379:88–91.
39. Fernandez-Checa JC, Kaplowitz N. Hepatic mitochondrial glutathione: transport and role in disease and toxicity. Toxicol Appl Pharmacol 2005;204:263–73.
40. Hashmi M, Graf S, Braun M, Anders MW. Enantioselective depletion of mitochondrial glutathione concentrations by (*S*)- and (*R*)-3-hydroxy-4-pentenoate. Chem Res Toxicol 1996;9:361–4.
41. Zhang WW, Churchill S, Lindahl R, Churchill P. Regulation of D-β-hydroxybutyrate dehydrogenase in rat hepatoma cell lines. Cancer Res 1989;49:2433–7.
42. Pennacchietti S, Michielli P, Galluzzo M, Mazzone M, Giordano S, Comoglio PM. Hypoxia promotes invasive growth by transcriptional activation of the met protooncogene. Cancer Cell 2003;3:347–61.
43. Selak MA, Armour SM, MacKenzie ED, et al. Succinate links TCA cycle dysfunction to oncogenesis by inhibiting HIF-α prolyl hydroxylase. Cancer Cell 2005;7:77–85.
44. Sato H, Sato M, Kanai H, et al. Mitochondrial reactive oxygen species and c-Src play a critical role in hypoxic response in vascular smooth muscle cells. Cardiovasc Res 2005;67:714–22.
45. Itoh S, Lemay S, Osawa M, et al. Mitochondrial Dok-4 recruits Src kinase and regulates NF-κB activation in endothelial cells. J Biol Chem 2005;280:26383–96.
46. Regula KM, Baetz D, Kirshenbaum LA. Nuclear factor-κB represses hypoxia-induced mitochondrial defects and cell death in ventricular myocytes. Circulation 2004;11:3795–802.
47. Wallace DA. mitochondrial paradigm of metabolic and degenerative diseases, aging, and cancer: a dawn for evolutionary medicine. Annu Rev Genet 2005;39:359–407.
48. Hampton MB, Orrenius S. Dual regulation of caspase activity by hydrogen peroxide: implications for apoptosis. FEBS Lett 1997;414:552–6.
49. Trachootham D, Zhou Y, Zhang H, et al. Selective killing of oncogenically transformed cells through a ROS-mediated mechanism by β-phenylethyl isothiocyanate. Cancer Cell 2006;10:241–52.
50. Pelicano H, Feng L, Zhou Y, et al. Inhibition of mitochondrial respiration: a novel strategy to enhance drug-induced apoptosis in human leukemia cells by a reactive oxygen species-mediated mechanism. J Biol Chem 2003;278:37832–9.